A Micromegas-based telescope for muon tomography: The WatTo experiment

S. Bouteille, D. Attié, P. Baron, D. Calvet, P. Magnier, I. Mandjavidze, S. Procureur, M. Riallot, M. Winkler

Nuclear Instruments and Methods in Physics Research A 834 (2016) 223–228

Contents lists available at ScienceDirect

Nuclear Instruments and Methods in Physics Research A

journal homepage: www.elsevier.com/locate/nima

A Micromegas-based telescope for muon tomography: The WatTo experiment

S. Bouteille [a], D. Attié [b], P. Baron [b], D. Calvet [b], P. Magnier [b], I. Mandjavidze [b], S. Procureur [a,*], M. Riallot [b], M. Winkler [b]

[a] CEA, Centre de Saclay, Irfu/SPhN, 91191 Gif sur Yvette, France
[b] CEA, Centre de Saclay, Irfu/Sedi, 91191 Gif sur Yvette, France

ARTICLE INFO

Article history:
Received 11 March 2016
Received in revised form
26 July 2016
Accepted 1 August 2016
Available online 2 August 2016

Keywords:
Genetic multiplexing
Micro Pattern Gaseous Detectors
MPGD
Micromegas
Muon Tomography
Volcanology
Muography

ABSTRACT

This paper reports about the first Micromegas-based telescope built for applications in muon tomography. The telescope consists of four, 50×50 cm^2 resistive multiplexed Micromegas with a 2D layout and a self-triggering electronics based on the Dream chip. Thanks to the multiplexing, the four detectors were readout with a single Front-End Unit. The high voltages were provided by a dedicated card using low consumption CAEN miniaturized modules. A nano-PC (Hummingboard) ensured the HV control and monitoring coupled with a temperature feedback as well as the data acquisition and storage. The overall consumption of the instrument yielded 30 W only, i.e. the equivalent of a standard bulb. The telescope was operated outside during 3.5 months to image the water tower of the CEA-Saclay research center, including a 1.5-month campaign with solar panels. The development of autonomous, low consumption muon telescopes with unprecedented accuracy opens new applications in imaging as well as in the field of muon metrology.

1. Introduction

1.1. Muon tomography

The muon tomography consists in imaging an object or a structure with muons produced in the atmosphere by highly energetic particles. It therefore uses a naturally available radiation, with large scanning capabilities. Muon tomography was shown to be a promising technique for more than 50 years (see e.g. [1–4]), but in practice the moderate muon flux[1] calls for two partially conflicting constraints:

- large detection areas;
- excellent spatial resolution to extract the most possible information from each recorded track.

Existing systems based on this technique often have to sacrifice one of these two criteria, with the consequence to have long scanning time or poor image quality.

Depending on the size and configuration of the studied structure, muon tomography can be operated in deviation mode or in absorption mode, as depicted in Fig. 1. If the object is small enough, detectors can be placed on its opposite sides[2] and the measurement of the upstream and downstream trajectory provides insights of the 3D density structure through the deviation angle due to multiple scattering. If the object is too large to be sandwiched by detectors, measurements are taken from only one side, and the flux deficit determines the integrated 2D density in the direction of observation. This mode requires much longer acquisition time, because of the fewer information available and because of the small absorption rate of cosmic muons.

1.2. Multiplexed micromegas

Micromegas detectors [5] have been developed initially for the needs of nuclear and particle physics. As other MPGDs, they offer in particular excellent spatial resolution thanks to their high granularity. Since their invention in 1996 their performance has been considerably improved—e.g. with the bulk technology [6] or the resistive strips [7]—resulting in robust and relatively cheap

* Corresponding author.
E-mail address: Sebastien.Procureur@cea.fr (S. Procureur).

[1] Roughly 150/m^2/s.

[2] Vertically, i.e. where the muon flux is maximal.

http://dx.doi.org/10.1016/j.nima.2016.08.002
0168-9002/

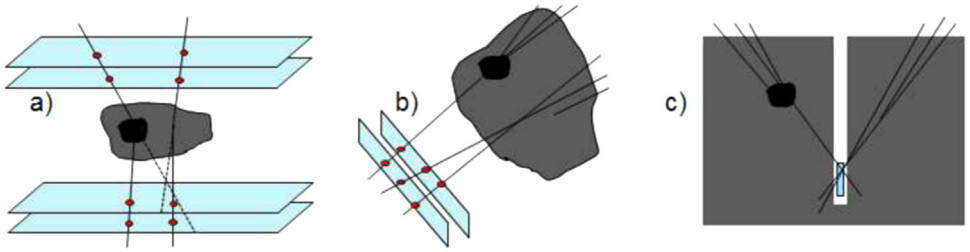

Fig. 1. Different modes of the muon tomography: particle deviation (a) and absorption (b and c).

detectors. Till recently, their application to muon tomography was however strongly limited by the enormous amount of readout electronics. This issue was solved by the invention of the genetic multiplexing [8] and large area 2D detectors with 2000 strips have been operated at full efficiency with only two 64-channel connectors [9]. The dramatic reduction of the electronics, of the consumption and of the cost of such systems now allows for the development of Micromegas-based muon telescopes with unprecedented accuracy for online imaging instruments. A first prototype was built at Saclay, and is presented in the next section.

2. The muon telescope

2.1. Detectors

The detection part is ensured by four multiplexed detectors with 2D readout (MG2D) and a 50×50 cm^2 active area, which were built at Cern. Though two detectors are a priori enough to reconstruct straight muon trajectories, this setup provides some redundancy for the self-triggering mode, double track reconstruction, calibration and alignment. Each detector was characterized in a cosmic test bench, with 2D efficiencies above 95%. Spatial resolutions of around 300 μm were measured while assembled in the telescope, corresponding to an angular resolution of 0.35 mrad (resp. 0.9 mrad) in the first (resp. second) phase of the experiment. The former value actually corresponds to the resolution blurring induced by the multiple scattering in the 7% X_0 telescope for a 10 GeV muon. The performance of the detectors is described in more details in [9]. For this experiment they were operated with a non-flammable, T2K-like gas mixture (Ar-Isobutane-CF_4 95–2–3%).

2.2. Electronics

A single 512-channel Front-End Unit (FEU) has been used for the readout of the four detectors of the telescope. The frontend electronics was primarily developed for the large chambers of the Clas12 Micromegas vertex tracker project [10]. The ability to remain efficient with highly capacitive detectors made the FEU well adapted to the muon telescope detectors with their huge ~1 nF channel capacitances due to the strong, 16–1 multiplexing factor. The FEU hosts eight 64-channel Dream [11] ASICs performing signal pre-amplification, shaping, sampling and buffering in a 512-cell deep analog memory per channel. A pair of Dream chips is connected to the *X* and *Y* detection planes of a Micromegas detector over 2 m long 64-channel micro-coaxial cables. The Dream chip can generate a fast hit signal when signal levels exceed a programmable threshold for a desired number of its input channels. An on-board FPGA device tracks the hit signals and initiates the readout of Dream chips when a software-set multiplicity criteria is satisfied within a coincidence time window. A desired number of analog samples corresponding to the trigger and completely containing the signals are digitized by the 8-channel flash ADC, further processed by the FPGA (including optional pedestal equalization, coherent noise subtraction and zero suppression), formatted and sent to the readout PC over a Gigabit Ethernet link. Thus for each trigger the complete signal shapes registered by all four detectors are available for further off-line processing allowing for more accurate analysis and signal to noise discrimination rather than binary *hit/no hit* information.

2.3. High voltages, PC and power supply

The high voltage power supply consists of five A7501 CAEN modules. These modules are made to output up to 2.1 kV at 100 μA from a 12 V input. We used one single negative module (A7501N) to supply the four cathodes to about −500 V (i.e. a 500 V/cm drift field). The four other modules were positive ones (A7501P), each supplying the resistive strips of a detector to about 470 V. To control these modules, a custom HVPS board was designed and built. This board can control up to 6 HV modules by setting the voltage, the maximum current and by monitoring the output voltage and current.

The telescope is supplemented by an acquisition computer to store the data and manage the runs. This is done by a HummingBoard, a nano-computer using an ARM processor (smartphone technology). It communicates with the FEU through an Ethernet interface, with the HVPS board through an SPI interface and with the outside world through a wired or wireless connection. A remote operation of the telescope is possible as well as retrieving the stored data since the Hummingboard have a limited capacity (of 32 GB) which can be extended by an external USB hard-drive.

All these components are powered by a 5 V input, with a 12 V/5 V converter if needed. This 12 V power input of the telescope makes it compatible with a wide range of common power supplies such as car/truck batteries or solar panels. The total power needed to operate the telescope is below 30 W which indeed easily allows for autonomous operation with standard solar panels. It should be emphasized that more than half of the required power is needed for the FEU which was originally designed for high flux experiments and large magnetic field environment.

2.4. Mechanics

The detectors and the electronic components were integrated in a Norcan-based mechanical structure shown in Fig. 2. Detectors are mounted on Aluminum plates which can be moved with plastic wheels on the main telescope axis to vary their relative distance up to roughly 1.5 m. Once positioned, they are further fixed by additional bars placed on top. The structure can be inclined from 0° to 55° above the horizon in steps of 5° and blocked with centering pins. The electronics is located downstream with either a battery or a 5 V power supply. Once ready, a protective, metallic cover is screwed and ensures the telescope to be water-proof and shielded. All in all, the telescope weights roughly 100 kg without the battery. A 20-liter bottle with pressurized detector gas is then fixed on its side with a flowmeter and a bubbler.

Fig. 2. Design of the WatTo telescope, represented here with only three detectors.

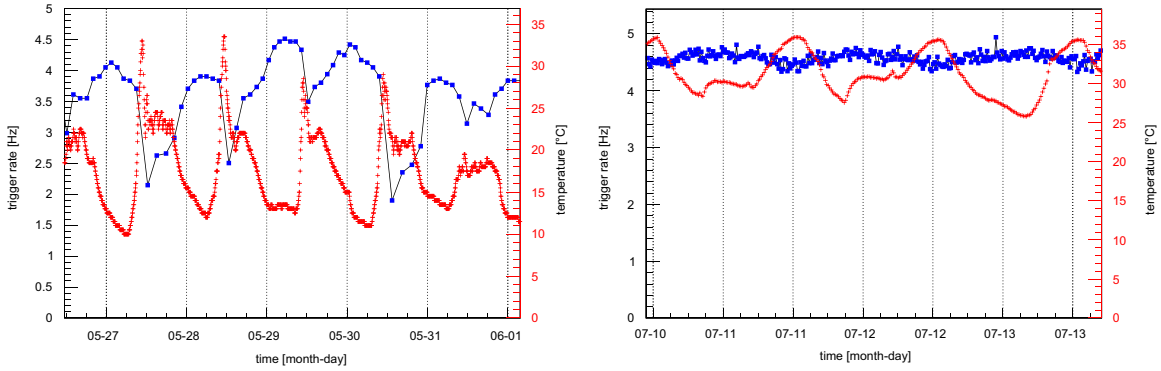

Fig. 3. Evolution of the trigger rate and of the temperature with time without (left) and with (right) the feedback on the high voltages. In the latter case, the trigger rate is practically constant.

3. The WatTo experiment

3.1. First phase

The telescope described in the previous section was installed in the vicinity of the CEA-Saclay water tower to check its imaging performance and validate its long term operation. Though it has been designed to be water-proof, internal safety rules required it to be covered by a tent. In the first phase, the telescope was located roughly 40 m away from the tower, nearby a building which provided us with the CEA network as well as electricity. In this configuration, the azimuthal angle was set at 30° with respect to the horizon and the distance between detectors to roughly 40 cm, with a total lever arm of 116.5 cm.

The thresholds for the self-triggering were fixed with strongly reduced high voltages for which the detection efficiency is very close to zero. Starting from the minimal values, these thresholds were increased until a negligible counting rate is obtained, typically less than 0.5 Hz. After increasing the high voltages at their nominal levels, a mean trigger rate of the order of 5 Hz was observed. In the following days, however, large fluctuations of the rate appeared, with a period of one day. It was rapidly realized that these fluctuations are highly anti-correlated with the temperature which affects the gain of the detectors, as shown in Fig. 3 (left). Indeed, a higher temperature leads to higher pressure which reduces the mean free path of electrons in the amplification gap, lowering the ionization probability[3] and the avalanche size. Though this is a general effect, it was not observed in the lab during the calibration process because of the relative indoors temperature stability. An online feedback of the high voltages of the detectors was therefore implemented as a function of the

[3] or equivalently the first Townsend coefficient

temperature recorded by the Hummingboard. Empirically, a slope of the order of 1.1 V/K was derived, which greatly stabilized the signal amplitude and the trigger rate, as can be seen in Fig. 3 (right). Because typical, relative pressure variations are roughly three times smaller than temperature ones, the corresponding effect was found to be small and not corrected for. However, a USB barometer was later purchased and an approximate feedback has been implemented after the water tower experiment. For the future experiments, tests will be made soon in a large oven to parametrize precisely the thermal effect.

3.2. Second phase

After 2 months of operation, the telescope was moved closer to the tower, and disconnected from the network and the mains supply. Two 150 W solar panels were installed outside the tent, and plugged to the instrument through a regulator and a 160 Ah truck battery. Because of several shadowing trees in the area as well as the tower itself and non-optimal pulse width modulation solar power controller, the boards were not enough to provide a full autonomy, and the system had to be switched off every week or so, depending on the weather.

In this completely different configuration, prohibitive noise levels for the self-triggering mode were observed. A 1 m-long Copper post was therefore planted in the soil, yielding a noise level before common mode subtraction 2–3 times higher than during the first phase. As a consequence, the purity of the trigger drops to roughly 50%, but without a significant change on its efficiency. In this configuration, the telescope angle was increased to 35° above the horizon. Last but not least, the lever arm was reduced to 45 cm with equally spaced detectors to increase the acceptance for simultaneous open sky measurements.

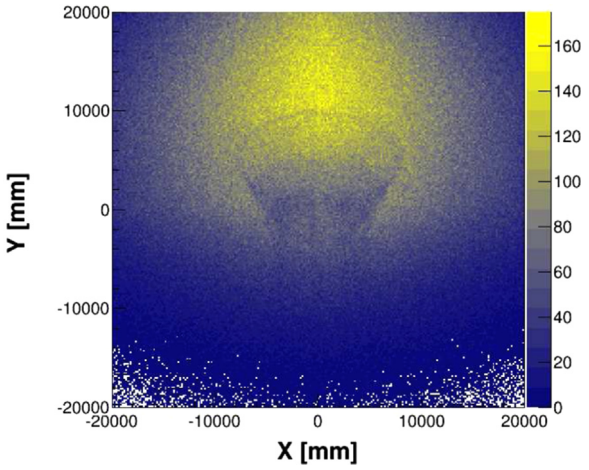

Fig. 4. Raw muography of the Saclay water tower with 4 weeks of data during the phase 1.

4. Performance and results

4.1. Static imaging

Muon tracks were reconstructed from the clusters obtained in the detectors after the demultiplexing process. Because of the redundancy, at least three clusters in the four detectors were required in each coordinate. The muography is then obtained from the accumulation of extrapolated positions of muons in the mid-plane of the water tower. Taking into account the angular resolution of the instrument (0.35 mrad) as well as the multiple scattering in the air (0.55 mrad) and in the telescope (0.35 mrad), the spatial resolution at the mid-plane is better than 5 cm. As shown in Fig. 4 (left) corresponding to 4 weeks of data taking in the first phase, several external architectural details of the water tower are visible, in particular the dome, the tank and concrete pillars. As expected, the water also appears clearly, with an absorption around 50%, representing around 10 m of water in addition to the concrete walls. At the center of the tank a brighter zone appears, corresponding to the central column of the tower containing the staircase. No correction has been applied on this image, which explains the general top-bottom and the center-edge asymmetries. The former originates from the $\cos^2$-like angular distribution of muons, while the latter is simply an acceptance effect. These two effects being very smooth, they do not degrade the image quality nor the detection of inhomogeneities.

During the second phase, the yearly emptying of the tower occurred and lasted 4 days during which another muography was taken. Fig. 5 shows the difference between a full and an empty tank. In the latter case, more details are revealed, in particular the concrete rings surrounding the conical tank.

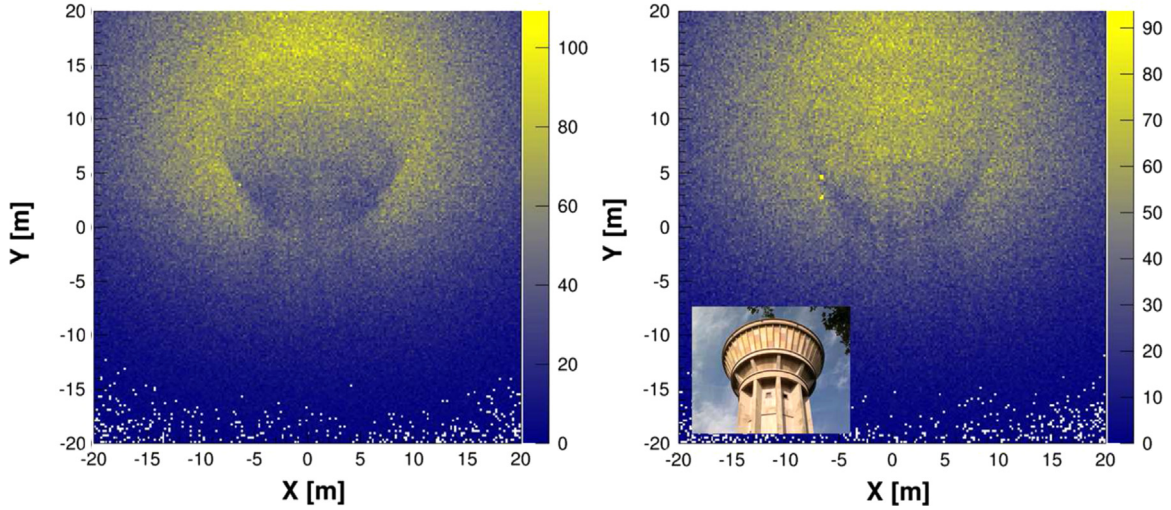

Fig. 5. Muography of the Saclay water tower with 4 days of data during the phase 2, with the water (left) and during the emptying (right).

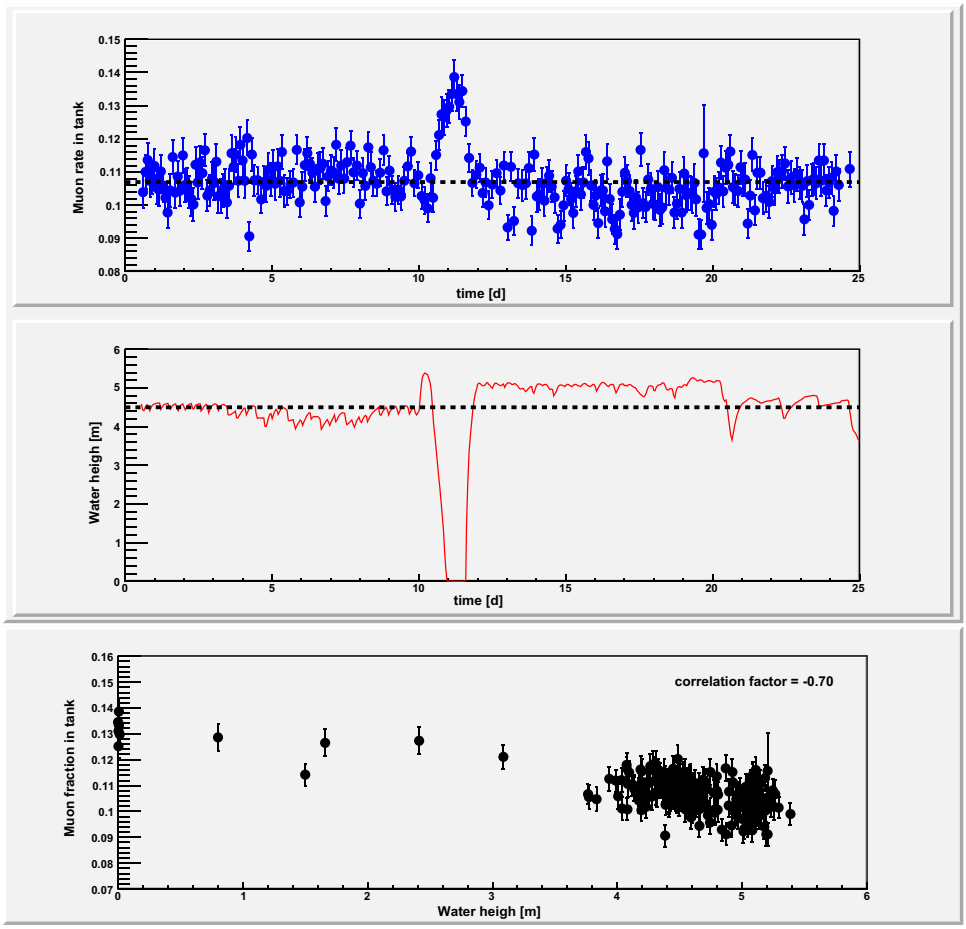

Fig. 6. (Top): relative inside muon flux evolution over a month of data during the phase 2. The muon flux inside the tank is divided by the flux measured outside. (Middle): the measured water level during the same period, including a draining of the tank. (Bottom): correlation between the relative inside muon flux and the water level.

4.2. *Dynamic imaging*

The Saclay water tower was actually chosen for its dynamic, the water level in the tank varying with time and being measured permanently. The ability to detect density variations is an essential feature of muon telescopes for many applications like volcanology, hydrology or metrology. The difficulty then consists in cancelling muon flux variations due to external reasons, like the environment (atmospheric pressure) or detector instabilities. It is worth mentioning that a similar experiment was conducted with a scintillator-based telescope inside a water tower [12]. In this case, the pressure effect could not be measured directly because of the limited acceptance of the instrument. In our case, however, the large acceptance gave us access to a large portion of open sky to measure the environmental variations. More precisely the ratio of muons passing inside and outside the water tank washes out both environmental and instrument variations. The inside of the water tank was defined as the region of the muography delimited by the upper dome and the visible concrete edges. This ratio is displayed in Fig. 6 over a month, and shows a strong anti-correlation with the water level. This proves in particular that the telescope can measure density fluctuations without any further external corrections.

5. Perspectives and conclusion

A Micromegas-based muon telescope was built and successfully operated outdoors for several months. The telescope benefitted from the intense R&D led on the last decade on MPGDs and their electronics resulting in robust and high-performance detectors. Thanks to the genetic multiplexing, the equipment and power consumption has been significantly reduced, and large area telescopes are now at hand for a reasonable price and unprecedented accuracy. A second version of the telescope is currently under development at Saclay with better spatial resolution, compactness and autonomy. It may be used in the coming months for the imaging of structures of archeological interest, or as a basis for a muon metrology instrument.

Acknowledgments

We are grateful to S. Rateau and V. Barriere for their help during the preparation of the experiment, in particular on the authorization and safety issues. We also deeply thank Y. Ambroise, B. Rousseau and S. Dezard who gave us access to their office and building for electricity and network connections during the first campaign of measurements.

References

[1] E.P. George, Commonw. Eng. (1955) 455.
[2] L.W. Alvarez, et al., Science 167 (1970) 832.
[3] K. Nagamine, et al., Nucl. Instrum. Methods Phys. Res. A 356 (1995) 585.
[4] E. Frlez, et al., Nucl. Instrum. Methods Phys. Res. A 440 (2000) 57.

[5] Y. Giomataris, et al., Nucl. Instrum. Methods Phys. Res. A 376 (1996) 29.
[6] Y. Giomataris, et al., Nucl. Instrum. Methods Phys. Res. A 560 (2006) 405.
[7] T. Alexopoulos, et al., Nucl. Instrum. Methods Phys. Res. A 640 (2011) 110.
[8] S. Procureur, R. Dupré, S. Aune, Nucl. Instrum. Methods Phys. Res. A 729 (2014) 888.
[9] S. Bouteille et al., Nucl. Instrum. Methods A, http://dx.doi.org/10.1016/j.nima.2016.08.006, in press.
[10] D. Attié et al., The Readout System for the Clas12 Micromegas Vertex Tracker, in: 19th IEEE Real-Time Conference, Nara, 2014.
[11] C. Flouzat et al., Dream: a 64-channel Front-end Chip with Analogue Trigger Latency Buffer for the Micromegas Tracker of the Clas12 Experiment, TWEPP conference, 2014.
[12] K. Jourde et al., arXiv:1504.02230 [physics.ins-det].